

# Morphology and Thermal and Mechanical Properties of Phosphonium Vermiculite Filled Poly(ethylene terephthalate) Composites

Xianshen Zeng,<sup>1</sup> Deming Cai,<sup>1</sup> Zhidan Lin,<sup>2</sup> Xiang Cai,<sup>1</sup> Xiuju Zhang,<sup>2</sup> Shaozao Tan,<sup>1</sup> Yingbin Xu<sup>3</sup>

<sup>1</sup>Department of Chemistry, Jinan University, Guangzhou 510632, People's Republic of China

<sup>2</sup>Department of Materials Science and Engineering, Jinan University, Guangzhou 510632, People's Republic of China

<sup>3</sup>Guangzhou Keyuan Innovative Materials Company, Limited, Guangzhou 510632, People's Republic of China

Received 30 May 2011; accepted 24 November 2011

DOI 10.1002/app.36553

Published online in Wiley Online Library (wileyonlinelibrary.com).

**ABSTRACT:** A series of poly(ethylene terephthalate) (PET)/phosphonium vermiculite (P-VMT) composites were prepared by a melt-blending method, and we investigated the morphology and thermal and mechanical properties of the composites. We prepared P-VMT with quaternary phosphonium salts using the common method followed by a cation-exchange reaction. X-ray diffraction showed that the phosphonium surfactants were partially intercalated into the vermiculite layers, The *d*-spacing of the PET-clay sample was somewhat less than that of the P-VMT because some degradation of the surfactant took place during melt processing. Compared with PET, the

PET-clay composites had a lower decomposition temperature and showed a 17.4% increase in the tensile strength with a P-VMT content of 3 wt %. Scanning electron microscopy and transmission electron microscopy demonstrated that P-VMT had a homogeneous dispersion and good compatibility in the polymer matrix with a low content of additive and indicated that the P-VMT content of 3 wt % was optimal. © 2012 Wiley Periodicals, Inc. *J Appl Polym Sci* 000: 000–000, 2012

**Key words:** composites; mechanical properties; morphology; organoclay; polyesters

## INTRODUCTION

Poly(ethylene terephthalate) (PET), a semicrystalline thermoplastic polymer with a high mechanical strength and solvent resistance, has become one of the most widely used polymers since it was first

prepared in 1946.<sup>1</sup> It is used in many fields, including textile fibers, films, containers, food-packaging materials, engineering plastics in automobiles, and electronics.<sup>2–7</sup> Also, it can be applied as an engineering plastic because of its good mechanical properties. Therefore, many efforts have been made to improve the mechanical, thermal, and other special properties. Among these efforts, polymer-clay composites have attracted much attention because they can have significantly improved properties of the polymer matrix with a very low content (usually <5 wt %) of clay.<sup>8–12</sup>

Litchfield DW<sup>13,14</sup> and his coworkers have studied the role of montmorillonite (MMT) in the generating process of PET fibers with improved modulus and tenacity. They found that the PET fibers showed 28 and 63% increases, respectively, in the Young's modulus and strength when a quaternary ammonium surface modified MMT with a 1 wt % content was added. Zeng and Bai<sup>15</sup> synthesized a PET/organomontmorillonite (OMMT) nanocomposite by *in situ* interlayers and found that the permeation of oxygen was reduced to half of that of the pure PET film when the OMMT content reached 3%. Wang et al.<sup>16</sup> found when the MMT content was 1%, the mechanical properties of their PET/MMT nanocomposites were the best. Rajeev et al.<sup>17</sup> studied the effect of equibiaxial stretching on the exfoliation of nanoclays

Correspondence to: S. Tan (shaozao@tom.com).

Contract grant sponsor: National Natural Science Foundation of China; contract grant numbers: 20871058, 21006038, 20971028.

Contract grant sponsor: Natural Science Key Foundation of Guangdong Province; contract grant number: 10251007002000000.

Contract grant sponsor: Foundation of Enterprise-University-Research Institute Cooperation from Guangdong Province and the Ministry of Education of China; contract grant number: 2008A010500005.

Contract grant sponsor: Foundation of Enterprise-University-Research Cooperation from Guangdong Province and the Chinese Academy of Sciences; contract grant number: 2010B090301036.

Contract grant sponsor: Foundation of Enterprise-University-Research from Huadou District; contract grant number: HD10CXY-G004.

Contract grant sponsor: Fundamental Research Funds for the Central University; contract grant number: 21610102.

in PET, and they found that the stretching ratio affected the properties, in that an increase in the stretching ratio improved the exfoliation of clay platelets. Calcagno et al.<sup>18</sup> found that tactoids in their PET/OMMT nanocomposites were obtained only when apolar modifiers were present. Barber et al.<sup>19</sup> and Ammala et al.<sup>20</sup> used an aqueous ionomer to improve the compatibility between PET and MMT. Davis's research group<sup>21</sup> investigated the effects of the processing conditions on the quality of PET/MMT nanocomposites. Some researchers have also focused on the effect of clays on the thermal stability of PET composites.<sup>22–24</sup> However, to the best of our knowledge, there are very few reports on PET/vermiculite (VMT) composites.<sup>25</sup>

In this study, quaternary phosphonium salt modified VMT was successfully prepared. Also, PET/phosphonium vermiculite (P-VMT) composites with three different P-VMT contents (1, 3, and 5 wt %) were prepared by the melt-mixing method. The effects of different organoclay contents on the morphological, thermal, and mechanical properties of PET were studied.

## EXPERIMENTAL

### Materials

PET was purchased from Far Eastern Industries, Ltd. (Shanghai, China). VMT, with a cation-exchange capacity of 135 mequiv/100 g, was purchased from Hebei Lingshou Micro-Mineral Co., Ltd. (Hebei, China) Butyl triphenyl phosphorane phosphorus chloride (BTP) was provided by Guangzhou Xiangrui Surfactant, Ltd., Co. (Guangzhou, China).

### Preparation of P-VMT

P-VMT was prepared with a BTP content of 1.5 cation-exchange capacity of VMT according to our previous work.<sup>26</sup> VMT was dissolved in 270 g of deionized water, to which the BTP was slowly added. Subsequently, the mixture was stirred vigorously at 60°C for 8 h. The resulting compound was washed with deionized water three times. After being dried at 80°C *in vacuo*, the layered compound was gathered with a 300-mesh sieve, and the resulting product was P-VMT.

### Preparation of the PET/P-VMT composites

PET composites consisting of 1, 3, and 5 wt % clay were prepared by melt mixing with a twin-screw extruder (SHJ-30 screw diameter = 30 mm, screw length = 120 cm, Nanjing, China). The screw speed was 150 rpm, and the mixed temperature was 260°C. The extrudates were pelletized, and the pellets were injection-molded into a standard spline with an injection-molding machine (HMT OENKEY,

Japan) with typical operating conditions: the feed opening temperature was 200°C, the barrel temperature was 270°C, the nozzle temperature was 260°C, and the temperature of the mold was maintained at room temperature. The samples were stored in a desiccator until they were tested.

### Analysis

UV spectroscopy was performed in the 200–800-nm wave-band range on a UV-visible near-infrared spectrophotometer (Cary 5000, USA). The X-ray diffraction (XRD) patterns were recorded on a Rigaku D/Max 1200 X-ray diffractometer (Geman) with Cu K $\alpha$  radiation ( $\lambda = 0.1541$  nm) at 36 kV and 20 mA with a scanning speed of 4°/min. Thermogravimetric analysis (TGA; SDT-Q600, TA Instruments, New castle, USA) studies were performed in an N<sub>2</sub> atmosphere between 70 and 650°C at a rate of 15°C/min. PET and its composites (0.25 g) were dissolved in a mixture of phenol and 1,1,2,2-tetrachloroethane (60 : 40 v/v) at 120°C for less than 0.5 h to avoid polymer degradation. After complete solubilization, the solutions were filtered and tested at 25°C in a water bath cylinder. The intrinsic viscosity ( $[\eta]$ ) and molecular weight were determined with the following equations<sup>27,28</sup>:

$$\eta_r = t/t_0 \quad (1)$$

$$[\eta] = \frac{25 \times (\eta_r - 1 + 3 \ln \eta_r)}{c} \quad (2)$$

Where  $\eta_r$  was relative viscosities,  $t$  is the flow time of the polymer solution (s),  $t_0$  is the flow time of the pure solvent mixture (s), and  $c$  is the polymer solution concentration (g/mL):

$$[\eta] = KM\alpha \quad (3)$$

The molecular weight was determined with the Mark-Houwink equation [eq. (3)], where  $K$  is 0.0468 mL/g, and  $\alpha$  is 0.68 ( $K$  and  $\alpha$  were specific for fixed conditions of polymer type, solvent and temperature). Measurement of the carboxyl terminal group content ([COOH]) was done by titration.<sup>27,29,30</sup> The samples (ca. 0.3 g) were dissolved in 10 mL of benzyl alcohol under a nitrogen atmosphere by being heated; they were then titrated with a 0.01N potassium hydroxide/glycol solution with phenol red as an indicator. The tensile tests were conducted with a universal testing machine (LLOYD LR100K, Britian). The conditions used for the measurements were room temperature and a crosshead speed of 50 mm/min. Scanning electron microscopy (SEM) images were observed with a JSM-6330F scanning electron microscope (Holand). We obtained cryogenically fractured surfaces by immersing the samples into



**Figure 1** Visual appearance of the PET/P-VMT composites. [Color figure can be viewed in the online issue, which is available at [wileyonlinelibrary.com](http://wileyonlinelibrary.com).]

liquid nitrogen for several minutes and breaking them with the tap of a hammer. All of the fracture surfaces were gold-coated before SEM examination. Transmission electron microscopy (TEM) was performed on Philips TECNAI-10 transmission electron microscope (Holand) with an accelerating voltage of 100 kV. Samples for TEM were prepared with ultramicrotome (Leica Ultracut UCT, Leica, Geman). Films with a thickness of around 70–100 nm were cut along the flow direction of the injection-molded tensile specimen with a freshly prepared glass knife.

## RESULTS AND DISCUSSION

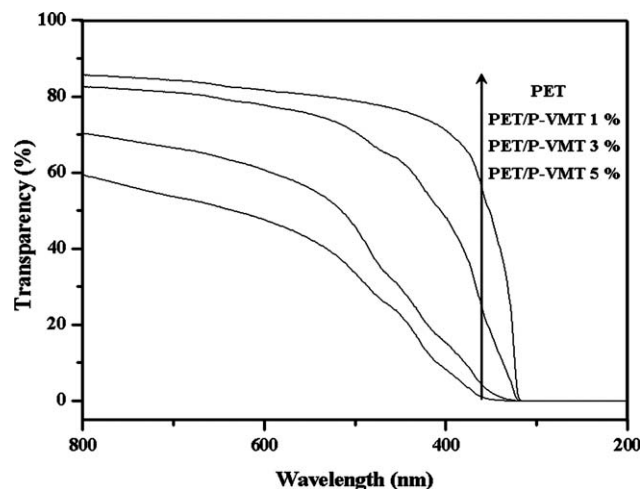
### Transparency of the PET and PET/P-VMT composites

Figure 1 shows the visual appearance of the PET/P-VMT composites. The photos were obtained with a digital camera. All of the samples were translucent (the size of each sample was 4.3 cm long, 3.2 cm wide, and 0.1 cm thick), and they became darker in color with increasing clay content. UV spectroscopy was used to determine the effect and light transmittance of the PET samples, as shown in Figure 2. The transmittances of pure PET were above 80%. When the wavelengths were in the range 400–800 nm, the light transmittance decreased with increasing con-

tent of clay. The light transmittance of the composite fell by almost 30% with the 5% addition of P-VMT.

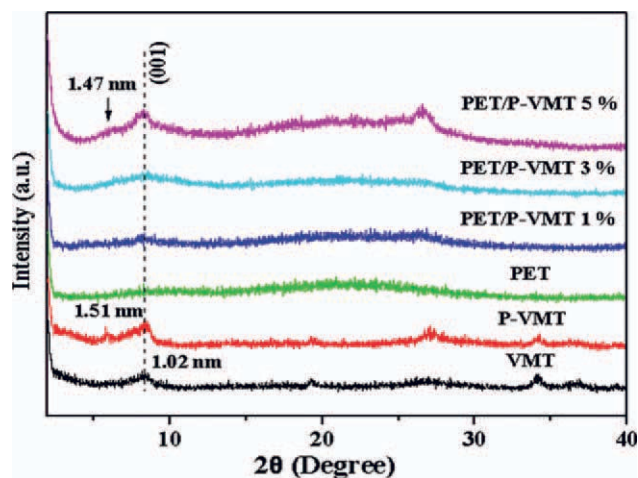
### XRD analysis

Figure 3 shows the XRD patterns of the clays and their composites with PET. The (001) plane of the VMT powder yielded a clear diffraction peak at



**Figure 2** UV spectra of the PET and PET/P-VMT composites.





**Figure 3** XRD patterns of the clays, PET, and PET/P-VMT composites. [Color figure can be viewed in the online issue, which is available at [wileyonlinelibrary.com](http://wileyonlinelibrary.com).]

$2\theta \approx 8.3^\circ$ ; this corresponded to a basal spacing of 1.02 nm. After modification with BTP, an additional basal spacing of 1.51 nm ( $2\theta \approx 6^\circ$ ) was observed; this suggested a partial incorporation of BTP inside the interlayer space. In the PET/P-VMT composites, a diffraction peak associated with P-VMT appeared at  $2\theta \approx 6.2^\circ$ ; this corresponded to a  $d$ -spacing of 1.47 nm, a value somewhat smaller than that of the P-VMT material. This result suggested that some degradation of the surfactant took place during the melt processing.

### Degradation behavior analysis

The TGA curves of the PET and PET–clay composites in a nitrogen environment are shown in Figure 4. Compared with the virgin PET, the PET–clay composites had lower decomposition tempera-

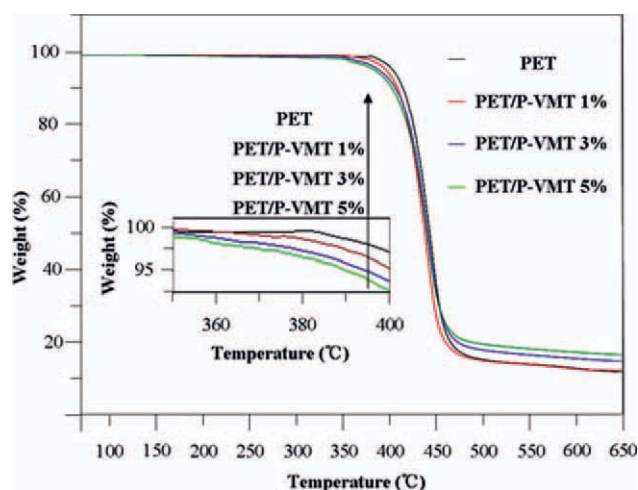


**Figure 4** TGA curves of the virgin PET and PET–clay composites under nitrogen. [Color figure can be viewed in the online issue, which is available at [wileyonlinelibrary.com](http://wileyonlinelibrary.com).]

**TABLE I**  
Viscosity, Molecular Weight, and [COOH] Values of the PET and PET–Clay Composites

Sample	$[\eta]$ (dL/g)	$M_w$ (g/mol)	[COOH] (mmol/kg)
PET	0.88	$65.17 \times 10^3$	42.48
PET + 1 wt % P-VMT	0.84	$60.99 \times 10^3$	45.73
PET + 3 wt % P-VMT	0.80	$57.04 \times 10^3$	51.36
PET + 5 wt % P-VMT	0.72	$48.76 \times 10^3$	60.24

tures; this was reflected in the onset decomposition temperature. This was probably due to the fact that the hydroxyl groups on the clays could accelerate the thermal decomposition of the PET matrix.<sup>31–35</sup>

Table I shows the  $[\eta]$ , weight-average molecular weight ( $M_w$ ), and carboxyl terminal group content values of the PET and PET/P-VMT composites. To exclude the factor of clays, all of the sample viscosity measurements were made with filtered solutions. The  $[\eta]$ , average molecular weight, and carboxyl terminal group content values of the pure PET were found to be 0.88 dL/g,  $65.17 \times 10^3$  g/mol, and 42.48 mmol/kg, respectively. Meanwhile, with increasing content of the clays,  $[\eta]$  and  $M_w$  decreased significantly,<sup>36</sup> whereas the content of carboxyl terminal groups increased. These data further confirmed the TGA results.

### Mechanical properties

The modulus, tensile strength, and strain at break data for the PET composites with different clay contents are summarized in Table II. The most striking result was that the P-VMT content exhibited a serious effect on the elongations at break of PET. The strain at break decreased with increasing clay content in the range of low clay contents, whereas the modulus of PET increased with increasing content of the clay. The tensile strength of the PET/P-VMT composites showed obvious change. When the addition of P-VMT was 3 wt %, the tensile strength was 64.8 MPa; this was a 17.4% increase.

The stress–strain curves of the PET and PET/P-VMT composites are shown in Figure 5. All of the curves had neckings, except that of PET/P-VMT 5%. This indicated that PET/P-VMT 5% was readily broken at a very low deformation. There was no doubt

**TABLE II**  
Characteristic Mechanical Properties of PET and Its Composites

PET (wt %)	P-VMT (wt %)	Modulus (MPa)	Tensile strength (MPa)	Strain at break (%)
100	0	523	55.2	490
99	1	540	59.6	350
97	3	706	64.8	120
95	5	753	42.3	5.4

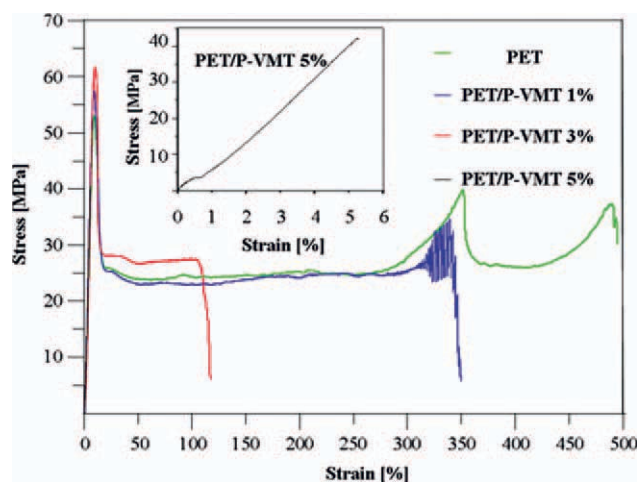


**Figure 5** Representative stress–strain curves of the PET and PET/P-VMT composites. [Color figure can be viewed in the online issue, which is available at [wileyonlinelibrary.com](http://wileyonlinelibrary.com).]

that P-VMT had poor dispersion in the polymer matrix, and it began to gather at this point.

#### Electron microscope analysis

The SEM images of the impact fracture surfaces of the PET and PET–clay composites shown in Figure 6 suggest that there was a rougher fracture surface at

a fine scale on the composite. We could see that there was clearly a much greater size of the holes when 5 wt % P-VMT was contained in PET; this indicated bad interfacial bonding between the clay and PET matrix. However, there are no significant differences between Fig. 6(b) and Fig. 6(c), and it's difficult to explain the previous mechanical properties results. Morphological analyses of the composites based on the tensile fracture surface of the PET and PET composites are shown in Figure 7. Except for that shown in Figure 7(d), the fracture surface tended to be better than that of PET. The average strip size of virgin PET was approximate 10  $\mu\text{m}$  [Fig. 7(a)], and the strips became smaller (average size <1  $\mu\text{m}$ ) when 1 wt % P-VMT was contained in PET. When the addition of P-VMT was 3 wt %, there were flocculent structures [magnified portion in Fig. 7(c)] on the fracture surface. PET containing 5 wt % P-VMT was characterized with a smooth surface and did not exhibit any strips. The SEM images of the fracture surfaces of the PET/P-VMT composites fully explained the previous mechanical properties results.

TEM is widely used to explore the dispersion effect of clays in polymers. As is shown in Figure 8, the clays in the PET composites did not exhibit any preferential orientation before tensile testing was conducted. In contrast, the TEM images of the necking of the PET/P-VMT composites clearly revealed

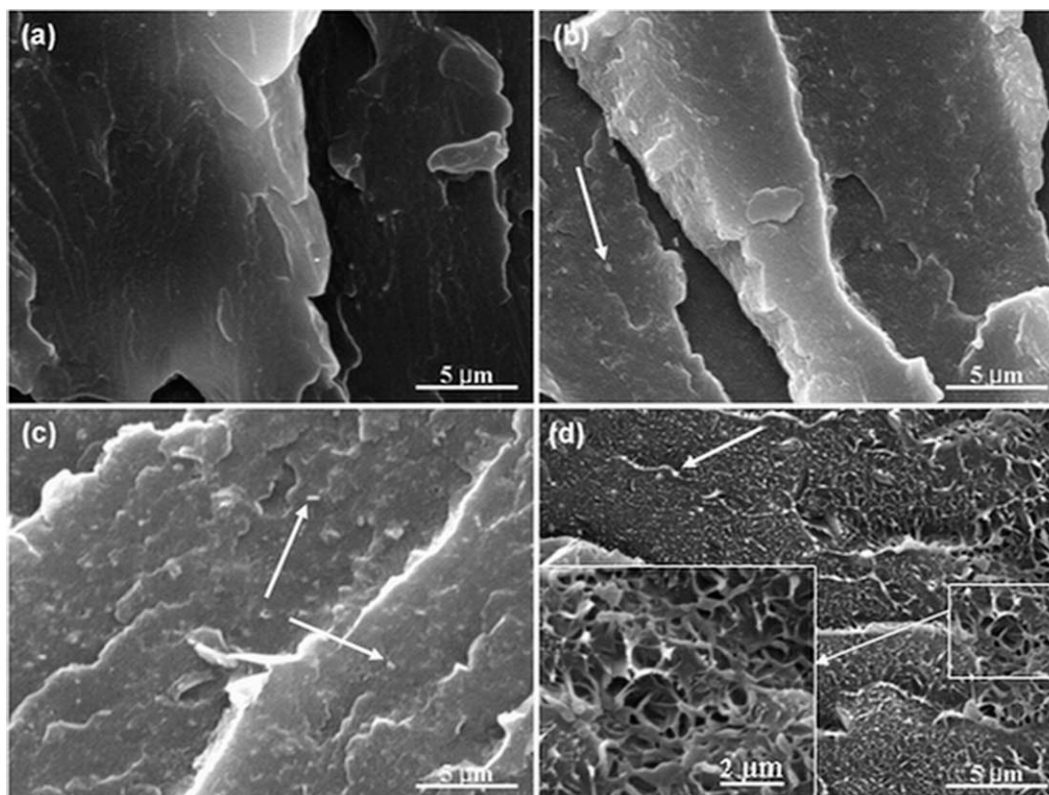


**Figure 6** Morphological analysis of composites based on cryogenic fracture surfaces of (a) PET with (b) 1, (c) 3, and (d) 5 wt % P-VMT contents. The arrows indicate P-VMT.



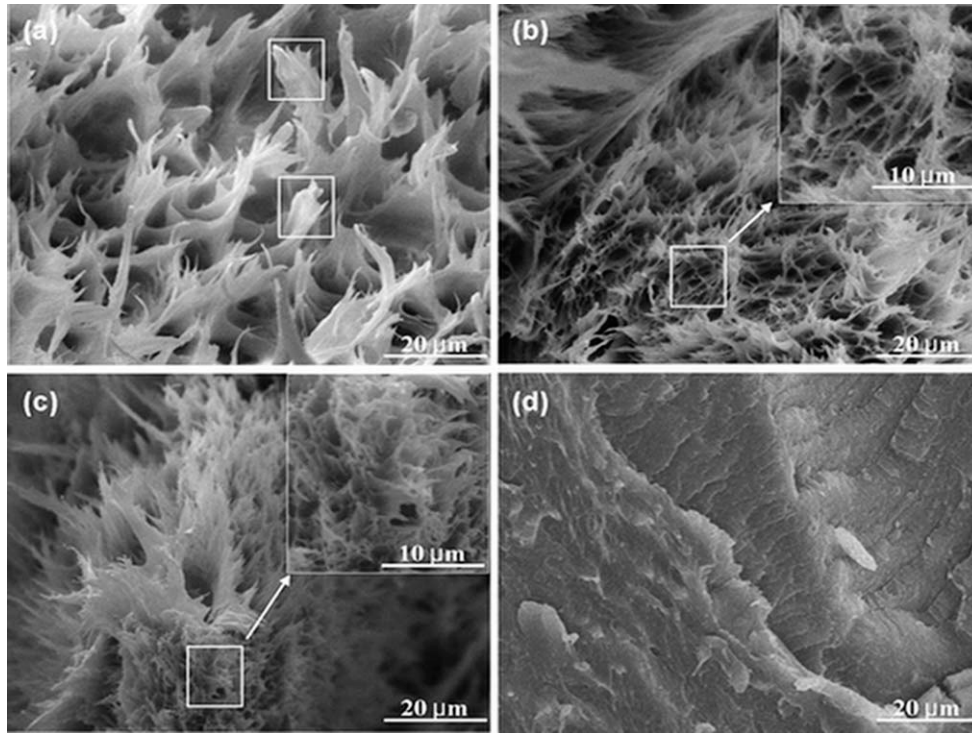


**Figure 7** Morphological analysis of composites based on the tensile fracture surfaces of (a) PET with (b) 1, (c) 3, and (d) 5 wt % P-VMT contents.

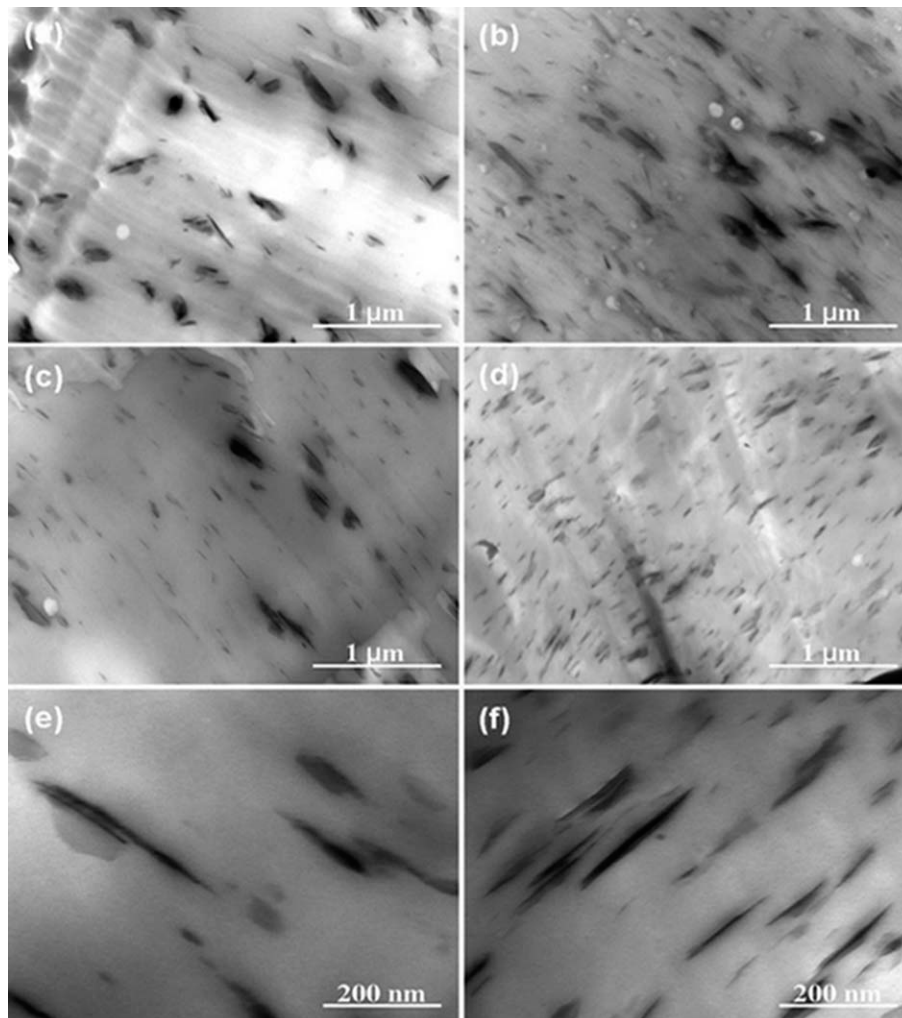


**Figure 8** TEM images of different PET–clay composites (a,b) without testing and (c–f) after tensile testing: (a) PET/1 wt % P-VMT, (b) PET/3 wt % P-VMT before testing, (c) PET/1 wt % P-VMT, (d) PET/3 wt % P-VMT after tensile testing, (e) PET/1 wt % P-VMT, and (f) PET/3 wt % P-VMT after tensile testing at high magnification.

an oriented distribution. Moreover, the dispersion effect of the clays in the PET matrix became better after tensile testing. This was due to the fact that the clays were forced to move with the PET molecule chain, and the mobility of the clays decreased with the strength of interaction.<sup>37</sup> It seemed that the interfacial interaction between the clays and PET was best when the P-VMT content was 3%.

## CONCLUSIONS

Quaternary phosphonium salt modified VMT was successful prepared, and PET/P-VMT composites with three different contents of P-VMT (1, 3, and 5 wt %, respectively) were prepared by the melt-mixing method. The light transmittance of the composites decreased with increasing content of clay. XRD showed an additional interlayer distance for P-VMT with respect to that observed for VMT; this suggested a partial incorporation of the surfactant within the clay platelets. Also, the *d*-spacing of the PET-clay sample was somewhat less than that of P-VMT because some degradation of the phosphonium surfactants took place during melt processing. The results of TGA, viscosity testing, and carboxyl terminal group contents of the PET and PET/P-VMT composites showed that the hydroxyl groups on the clays accelerated the thermal decomposition of the PET matrix.

The strain at break decreased with increasing content of clay in the range of low clay contents, and the modulus of PET increased with increasing content of the clay. Compared with PET, the PET/P-VMT composites showed obvious change. When the addition of P-VMT was 3 wt %, the tensile strength showed a 17.4% increase.

SEM images showed that the morphology of the cryogenic fracture surfaces became coarser with increasing clay content and showed small cavities when the addition of P-VMT was 5%. The morphological analysis of the composites based on the tensile fracture surfaces of the PET and PET composites showed that when the addition of P-VMT was less than 5%, the fracture surface tended to be better than that of pure PET. PET containing 5 wt % P-VMT was characterized with a smooth surface and did not exhibit any strips.

On the basis of the obtained results, the influence on the mechanical properties of the composites could be ascribed mainly to homogeneous dispersion and interactions between both components. Meanwhile, PET with 3 wt % P-VMT balanced the mechanical properties wonderfully.

## References

- Whinfield, J. R.; Dickinson, J. T. U.K. Pat. 578,079 (1946).
- Dinelli, F.; Assender, H. E.; Kirov, K.; Kolosov, O. V. *Polymer* 2000, 41, 4285.
- Hsu, Y. G.; Su, X. W.; Lin, K. H.; Wan, Y. S.; Chen, J. C.; Guu, J. A.; Tsai, P. C. *J Appl Polym Sci* 2011, 119, 693.
- Xue, G.; Ji, G. D.; Yan, H.; Guo, M. M. *Macromolecules* 1998, 31, 7706.
- Guan, R.; Wang, B. Q.; Lu, D. P. *J Appl Polym Sci* 2003, 88, 1956.
- Takahashi, Y.; Sakuma, K.; Itai, T.; Zheng, G. D.; Mitsunobu, S. *Environ Sci Technol* 2008, 42, 9045.
- Zhang, H. B.; Zheng, W. G.; Yan, Q.; Yang, Y.; Wang, J. W.; Lu, Z. H.; Ji, G. Y.; Yu, Z. Z. *Polymer* 2010, 51, 1191.
- Kiliaris, P.; Papaspyrides, C. D. *Prog Polym Sci* 2010, 35, 902.
- Kumara, A. P.; Depana, D.; Tomerb, N. S.; Singha, R. P. *Prog Polym Sci* 2009, 34, 479.
- Michael, A.; Philippe, D. *Mater Sci Eng R* 2000, 28, 1.
- Ross, E.; Behling, L. M.; Cochran, E. W. *Macromolecules* 2010, 43, 2111.
- Gournis, D.; Jankovič, L.; Maccallini, E.; Benne, D.; Rudolf, P.; Colomer, J. F.; Sooambar, C.; Georgakilas, V.; Prato, M.; Fanti, M.; Zerbetto, F.; Sarova, G. H.; Guldi, D. M. *J Am Chem Soc* 2006, 128, 6154.
- Litchfield, D. W.; Baird, D. G. *Polymer* 2008, 49, 5027.
- Litchfield, D. W.; Baird, D. G.; Rim, P. B.; Chen, C. *Polym Eng Sci* 2010, 50, 2205.
- Zeng, K.; Bai, Y. P. *Mater Lett* 2005, 59, 3348.
- Wang, Y. M.; Gao, J. P.; Ma, Y. Q.; Agarwal, U. S. *Compos B* 2006, 37, 399.
- Rajeev, R. S.; Harkin-Jones, E.; Soon, K.; McNally, T.; Menary, G.; Armstrong, C. G.; Martin, P. J. *Eur Polym J* 2009, 45, 332.
- Calcagno, C. I. W.; Mariani, C. M.; Teixeira, S. R.; Mauler, R. S. *Polymer* 2007, 48, 966.
- Barber, G. D.; Calhoun, B. H.; Moore, R. B. *Polymer* 2005, 46, 6706.
- Ammala, A.; Bell, C.; Dean, K. *Compos Sci Technol* 2008, 68, 1328.
- Davis, C. H.; Mathias, L. J.; Gilman, J. W.; Schiraldi, D. A.; Shields, J. R.; Trulove, P.; Sutto, T. E.; Delong, H. C. *J Polym Sci Pol Phys* 2002, 40, 2661.
- Chang, J. H.; Kim, S. J.; Joo, Y. L.; Im, S. *Polymer* 2004, 45, 919.
- Ou, C. F.; Ho, M. T.; Lin, J. R. *J Appl Polym Sci* 2004, 91, 140.
- Chung, J. W.; Son, S. B.; Chun, S. W.; Kang, T. J.; Kwak, S. Y. *Polym Degrad Stab* 2008, 93, 252.
- Kravitz, H. S.; Levitt, F. U.S. Pat. Appl. 254160 (2007).
- Yu, B.; Zeng, X. S.; Dai, G. J.; Cai, X.; Lin, Z. D.; Zhang, X. J.; Tan, S. Z.; Liu, Y. L. *Asian J Chem* 2011, 23, 2069.
- Xu, X. F.; Ding, Y. F.; Qian, Z. Z.; Wang, F.; Wen, B.; Zhou, H.; Zhang, S. M.; Yang, M. S. *Polym Degrad Stab* 2009, 94, 113.
- Sanches, N. B.; Dias, M. L.; Pacheco, E. B. *Polym Test* 2005, 24, 688.
- Berti, C.; Bonora, V.; Colonna, M.; Lotti, N.; Sisti, L. *Eur Polym J* 2003, 39, 1595.
- Pilati, F.; Toselli, M.; Messori, M.; Manzoni, C.; Turturro, A.; Gattiglia, E. G. *Polymer* 1997, 38, 4469.
- Shen, Y. C.; Eileen, H. J.; Hornsby, P.; Tony, M. N.; Rund, A. Z. *Compos Sci Technol* 2011, 71, 758.
- Stoeffler, K.; Lafleur, P. G.; Denault, J. *Polym Degrad Stab* 2008, 93, 1332.
- Xu, X. F.; Ding, Y. F.; Wang, F.; Wen, B.; Zhang, J. H.; Zhang, S. M.; Yang, M. S. *Polym Compos* 2010, 31, 825.
- Yuan, X. P.; Li, C. C.; Guan, G. H.; Xiao, Y. N.; Zhang, D. J. *Polym Degrad Stab* 2008, 93, 466.
- Yuan, X. P.; Li, C. C.; Guan, G. H.; Xiao, Y. N.; Zhang, D. J. *J Appl Polym Sci* 2008, 109, 4112.
- Patro, T. U.; Khakhar, D. V.; Misra, A. *J Appl Polym Sci* 2009, 113, 1720.
- Deepak, S.; Pralay, M.; Jiang, D. D.; Batt, C. A.; Giannelis, E. P. *Adv Mater* 2005, 17, 525.